Magnetic Susceptibility Calculated from Correlation-Lengths Derived by Mössbauer Relaxation Spectra

J. Pebler, C. Frommen, M. Mangold, and W. Treutmann[a]

Fachbereiche Chemie und Geowissenschaften[a] der Philipps-Universität
und Wissenschaftliches Zentrum für Materialwissenschaften, D-35032 Marburg

Reprint request to Prof. J. P.; Fax: 06421-28-8917

Z. Naturforsch. **54a**, 317–328 (1999); received March 17, 1999

From the knowledge of the spin correlation functions derived from Mössbauer relaxation spectra of quasi-one-dimensional $A_2Mn_{0.98}Fe_{0.02}F_5(H_2O)$ we could fit the antiferromagnetic susceptibilities of $A_2MnF_5(H_2O)$ with $A = Na^+$, $(NH_4)^+$, K^+, Rb^+ obtained for single crystal samples. The calculation yielded characteristic parameters such as the local anisotropy D, the intra-chain exchange energy J, the inter-chain exchange energy $|J'|$, the Néel temperature T_N, and the spin canting angle φ.

Key words: Mössbauer Relaxation Spectra; Non-linear Excitations (Magnetic Solitons); 1-d Correlation Length; Exchange and Anisotropy Energy; Antiferromagnetic Order; Weak Ferromagnetism.

Introduction

In the following we present efforts to calculate the magnetic susceptibility from experimentally determined spin correlation lengths in 1-d fluoromanganates(III), and we will discuss results for the antiferromagnetically ordered compounds $A_2MnF_5(H_2O)$ and $AMnF_5(H_2O)$ with A = Na, NH_4, K or Rb and A = Sr, Ba or enH_2, respectively [1–5]. In the light of this discussion, we will get back to previously reported studies of the ^{57}Fe Mössbauer effect in the iron-doped compounds of $A_2Mn_{0.98}Fe_{0.02}F_5(H_2O)$ and $AMn_{0.98}Fe_{0.02}F_5(H_2O)$ [6–12], where we investigated the spin-dynamics and non-linear excitations (solitons) in these compounds. From the analysis of Mössbauer relaxation spectra based on the classical soliton model [13–18] we were able to determine the activation energy for such a soliton from the temperature dependence of the spin-fluctuation rate in the antiferromagnetic 1-d phase even of powder samples [8–10, 12, 19–21].

Structural Properties of $A^I_2/A^{II}MnF_5(H_2O)$

The Jahn-Teller theorem is applicable to the degenerate ground state of manganese(III) complexes with octahedral symmetry. In case of Mn^{3+} ($3d^4$) with $S = 2$, the $^5D_0$ term is split in an octahedral field to yield a ^5E_g ground state and a $^5T_{2g}$ excited state [22, 23]. If the octahedral symmetry of the ligand field is reduced by the Jahn-Teller effect to axial symmetry, (the octahedra are remarkably lengthened in the bridging direction), the orbital degeneracy of the ^5E_g ground state is removed. If the x and y axes point at the in-plane fluorine ligands, the d-orbitals will be arranged such that d_{xz}, and d_{yz} remain degenerate, followed by d_{xy} and d_{z^2} and finally by $d_{x^2-y^2}$ as the most destabilized antibonding orbital. For a compressed octahedral arrangement the $d_{x^2-y^2}$ orbital is stabilized. In this scheme the four 3d-electrons will generate a $^5B_{1g}$ or $^5A_{1g}$ ground state for axially elongated or compressed octahedra, respectively [11].

When mixing of the ground and excited states becomes important, the susceptibilities differ from the spin-only prediction and become anisotropic due to the existence of a local anisotropy (zero-field splitting) [8].

A common feature of all fluoromanganates(III) with the general formula $A^I_2/A^{II}MnF_5(H_2O)$ is that they are built from infinite chains of trans corner-linked $[MnF_4F_{2/2}]^{2-}$ octahedra, with individual chains being separated by alkaline (A^+) or earth alkaline (A^{2+}) ions [11]. In our case of $A_2MnF_5(H_2O)$ these counter-ions are Na^+, $(NH_4)^+$, K^+, and Rb^+. Due to the Jahn-Teller effect, the long axial Mn-F_{ax} bonds of the distorted $[MnF_4F_{2/2}]^{2-}$ octahedra all lie along the chain direction, which yields a ferrodistortive [32] arrangement. An increase in size of the counter-ion results in a widening of the (Mn-F_{ax}-Mn) bridging angle γ from 132.5° for Na_2MnF_5 to 175.4° for $Rb_2MnF_5(H_2O)$ (see Table 1) [3]. The coordination around Mn(III) is very nearly axially symmetric (D_{4h}). The EPR-spectra for a single crystal of

0932-0784 / 99 / 0500-0317 $ 06.00

Table 1. Structural data in the following order: Mn-F-Mn bridge angle γ, Mn-Mn intrachain distance, Mn′-Mn interchain distance, Mn-F terminal bond Mn_{eq}, the Mn-F bridge bond Mn_{ax}, and the space group SG.

Compound	γ[°]	M-M [Å]	M′-M [Å]	M_{eq} [Å]	M_{ax} [Å]	SG	Ref.
Na_2MnF_5	132.5	3.860	5.236 (2×) 6.029 (4×)	1.851	2.103	$P2_1/c$	[3, 24]
$(NH_4)_2MnF_5$	139.4	3.974	6.199 (4×) 6.232 (2×)	1.844	2.114	Pnma	[3, 25, 26]
$(ND_4)_2MnF_5$	139.5	3.973	6.199 (4×) 6.227 (2×)	1.841	2.118	Pnma	[27, 28]
enH_2MnF_5	159.5	4.239	6.153(2×) 6.260 (2×)	1.838	2.154	Cccm	[5, 10]
$K_2MnF_5(H_2O)$	163.2	4.107	6.000 (2×) 6.123 (2×)	1.846	2.076	$P2_1/m$	[3, 29, 30]
$Rb_2MnF_5(H_2O)$	175.4	4.174	6.235 (2×) 8.002 (2×) 9.383 (2×)	1.848	2.089	Cmcm	[3, 31]

$(NH_4)_2MnF_5$ (space group Pnma, $Z=4$) were found to be nearly isotropic with signals at g values of $g_\perp=2.002$ and $g_{||}=1.997$ [33].

For orthorhombic symmetry, the influence of zero-field splitting on the measurable magnetic properties can be accounted for by addition of two terms to the isotropic exchange interaction. The Hamiltonian for the single chain in a magnetic field may be written in the form

$$\hat{\mathcal{H}} = \sum \left\{ -2J S_i S_{i+1} + D\left(S_{i,z}^2 - \frac{1}{3} S_i (S_i+1) \right) + E (S_{i,x}^2 - S_{i,y}^2) - g \mu_B H S_i \right\}, \quad (1)$$

where S and S_ν ($=x, y, z$) are spin operators related to the actually occupied energy levels. The chain direction is along the z axis. The first term in (1) represents an isotropic Heisenberg exchange interaction between two neighbouring spins in the chain. D and E are the axial and orthorhombic crystal field parameters. The single-ion-type anisotropy may arise from the crystal potential. Since the equatorial Mn-F_{eq} distances in the plane perpendicular to the z axis differ only by less than 0.1% we will neglect the orthorhombic anisotropy E (third term in (1)) in our discussion. The fourth term in (1) represents the Zeeman-interaction.

As has previously been shown for Mn(III) chain compounds of the type $A^I{}_2/A^{II}MnF_5(H_2O)$ [21], it follows that $|D| \gg E$ and $|J| > |D|$. The model given in (1) is therefore a valid approximation to describe the properties of a 1-d Mn^{3+} magnetic system.

Correlation Length

In previous papers [6–12, 19–21] we demonstrated that Mössbauer spectroscopy is a suitable method to study non-linear excitations in one-dimensional antiferromagnetic chain compounds of $A^I{}_2Mn(III)_{0.98}Fe(III)_{0.02}F_5(H_2O)$ and $A^{II}Mn(III)_{0.98}Fe(III)_{0.02}F_5(H_2O)$.

The characteristic Mössbauer parameters as quadrupole splitting and magnetic hyperfine field H are listed in Table 2 or are given in [6–12, 19–21]. The detailed theoretical analysis of domain wall dynamics and solitons in magnetic chains with a large local anisotropy D shows that, in a certain range above the critical temperature T_N, the density of π domain walls and their motion determines the spin autocorrelation function $\langle \boldsymbol{S}(0)\boldsymbol{S}(t)\rangle$, which is obtained by measuring the fluctuating hyperfine field $\boldsymbol{H}(t) \propto \boldsymbol{S}(t)$. The temperature dependence of the Mössbauer spectra for a representative powder sample of $(NH_4)_2Mn_{0.98}Fe_{0.02}F_5$ (one of ten investigated fluoromanganates(III) compounds) is shown in Figure 1. The Mössbauer spectra could successfully be fitted, as for all other compounds, by adopting the Blume Tjon relaxation model [34–36], in which it is assumed that the hyperfine field jumps stochastically with a flipping rate Γ between the two possible value $+H_{hf}$ and $-H_{hf}$. This takes into account a time-dependent Hamiltonian [36]. Thus, the hf interaction is replaced by a fluctuating effective field, and the increase in the fluctuation rate causes line broadening, asymmetric spectra, and related phenomena [16]. In doing so, the Mössbauer spectra could be fully fitted at all temperatures, with the spin fluctuation rate Γ and the ratio of the probabilities that $+H_{hf}$ jumps to $-H_{hf}$ and vice versa, as the only adjustable, temperature-dependent parameters.

Table 2. Experimentally determined parameters in the following order: complementary angle δ by X-ray diffraction [3], static Mössbauer parameters of the magnetic hyperfine field H_{hf}, the quadrupole splitting ΔE^Q at 4.2 K, and the calculated thermal activation energy E_A/k from the relaxation spectra on the basis of the classical soliton theory. Parameters obtained by measurements on powders and single crystals for the 1-d antiferromagnetic intrachain exchange constant J and the soliton energy E_s, the anisotropy constant D, the Néel temperature T_N, the interchain exchange constant J', the ratio J'/J and the canting angle φ derived from (15), respectively. The anisotropy constants in Table 2 are to compare with the averaged value $D/k = 2.75(3)$ K derived from Mössbauer spectroscopy (see Figure 3).

Compound	X-ray	Mössbauer effect measurements on powders			Magnetic single crystal measurements						
	$\delta = (180-\gamma)/2$ [°]	H_{hf} [kOe]	ΔE^Q [mm/s]	E_A/k [K]	J/k [K]	E_s/k [K]	D/k [K]	T_N [K]	$\lvert J'\rvert$ [K]	$\lvert J'/J\rvert$	φ_M [°]
Na_2MnF_5	23.8	545(3)	1.118(7)	140(3)	−8.8(2)	70(1)	−2.85(5)	9.2(3)	$1.4 \cdot 10^{-3}$	$1.6 \cdot 10^{-4}$	5(2)
$SrMnF_5(H_2O)$	20.1	542(3)	0.790(7)	158(3)	−10.1(2)*)	–	–	8.1(3)	$2.2 \cdot 10^{-3}$	$2.1 \cdot 10^{-4}$	–
$(NH_4)_2MnF_5$	20.3	525(3)	0.720(5)	166(3)	−10.6(2)	86(1)	−2.80(5)	8.5(3)	$2.7 \cdot 10^{-4}$	$2.6 \cdot 10^{-5}$	4(1)
$(ND_4)_2MnF_5$	20.3	527(3)	0.723(7)	163(3)	−10.3(1)	85(1)	2.74(5)	9.0	$2.7 \cdot 10^{-4}$		4.6
$BaMnF_5(H_2O)$	16.2	528(3)	0.835(5)	170(4)	−12.8(2)*)	–	–	11.5(5)	$2.7 \cdot 10^{-3}$	$2.1 \cdot 10^{-4}$	–
enH_2MnF_5	10.3	532(3)	0.991(6)	184(3)	−13.6(2)	95(2)	−2.82(5)	14.5(5)	$5.5 \cdot 10^{-3}$	$4.1 \cdot 10^{-4}$	2(1)
$K_2MnF_5(H_2O)$	8.4	535(3)	0.799(7)	209(4)	−17.0(2)	102(2)	−2.73(5)	14.5(5)	$7.5 \cdot 10^{-3}$	$4.4 \cdot 10^{-4}$	1(1)
$Rb_2MnF_5(H_2O)$	2.3	521(3)	0.840(5)	234(5)	−20.0(2)	122(2)	−2.80(5)	22.8(3)	$1.6 \cdot 10^{-2}$	$8.3 \cdot 10^{-4}$	0(1)
$Cs_2MnF_5(H_2O)$	0.0	525(3)	0.850(5)	–	−17.8(3)*)	–	–	16.5(5)			–

*) Powder sample.

Based on the classical soliton theory [16, 37–45] we discussed and analyzed the spin fluctuation rates Γ for $NaMn_{0.98}Fe_{0.02}F_5$ [12], $(NH_4)_2Mn_{0.98}Fe_{0.02}F_5$ [9], $enH_2Mn_{0.98}Fe_{0.02}F_5$ [10], $K_2Mn_{0.98}Fe_{0.02}F_5(H_2O)$, and $Rb_2Mn_{0.99}Fe_{0.01}F_5(H_2O)$ [8]. We want to emphasize that a feature of our experimental results is the observation of two subspectra, each of which shows a separate relaxation mechanism. Approaching the magnetically split phase from above one observes the apparent coexistence of contributions from the paramagnetic and magnetically ordered phase. This transition is accompanied by slow and fast relaxation phenomena, which may be attributed to non-linear excitations of domain walls. This unusual behaviour is observed in $(NH_4)_2Mn_{0.98}Fe_{0.02}F_5$ between 9 and 13 K (Figure 1). There appears a central asymmetric doublet due to faster relaxation. Above 13 K, the intensity of the slowly relaxing subspectrum becomes negligible, such that only a single spectrum is sufficient to fit the experiment. These features were in common for all our samples studied by Mössbauer spectroscopy and were also observed by de Jongh and his group [16–18]. The Mössbauer spectra were assumed to consist of two subspectra with equal static parameters but different relaxation rates.

To obtain the fliprate Γ from the measured spectra we have employed, as mentioned above, the Blume and Tjon model. The spin fluctuation rate Γ is defined as (see for example de Groot [16])

$$\Gamma = 2 n_s v_s = v_s \xi^{-1}, \tag{2}$$

where n_s is the soliton density,

$$n_s = \sqrt{\frac{8}{\pi}} \cdot \frac{1}{d} \cdot \sqrt{\frac{E_s}{kT}} \exp\left(\frac{-E_s}{kT}\right), \tag{3}$$

v_s the soliton velocity:

$$v_s = \frac{4|J|S}{\sqrt{\frac{E_s}{2kT}}}, \tag{4}$$

d the width of a domain wall:

$$d = \frac{4|J|S^2}{E_s} = \sqrt{\frac{|J|}{|D|}}, \tag{5}$$

and E_s is the soliton energy:

$$E_s = 4S^2 \sqrt{|D \cdot J|}. \tag{6}$$

For the inverse correlation length ξ^{-1} (see (2)) it follows that

$$\xi^{-1} = 2 n_s = 2 \cdot \sqrt{\frac{8}{\pi}} \cdot \frac{1}{d} \cdot \sqrt{\frac{E_s}{kT}} \exp\left(\frac{-E_s}{kT}\right). \tag{7a}$$

Therefore the spin fluctuation rate Γ derived from the Mössbauer spectra can be expressed by

$$\Gamma = 2 n_s v_s = \frac{2^5}{\sqrt{\pi}} J \cdot S \sqrt{\frac{D}{J}} \cdot \exp\left[-\frac{E_A}{kT}\right]. \tag{8}$$

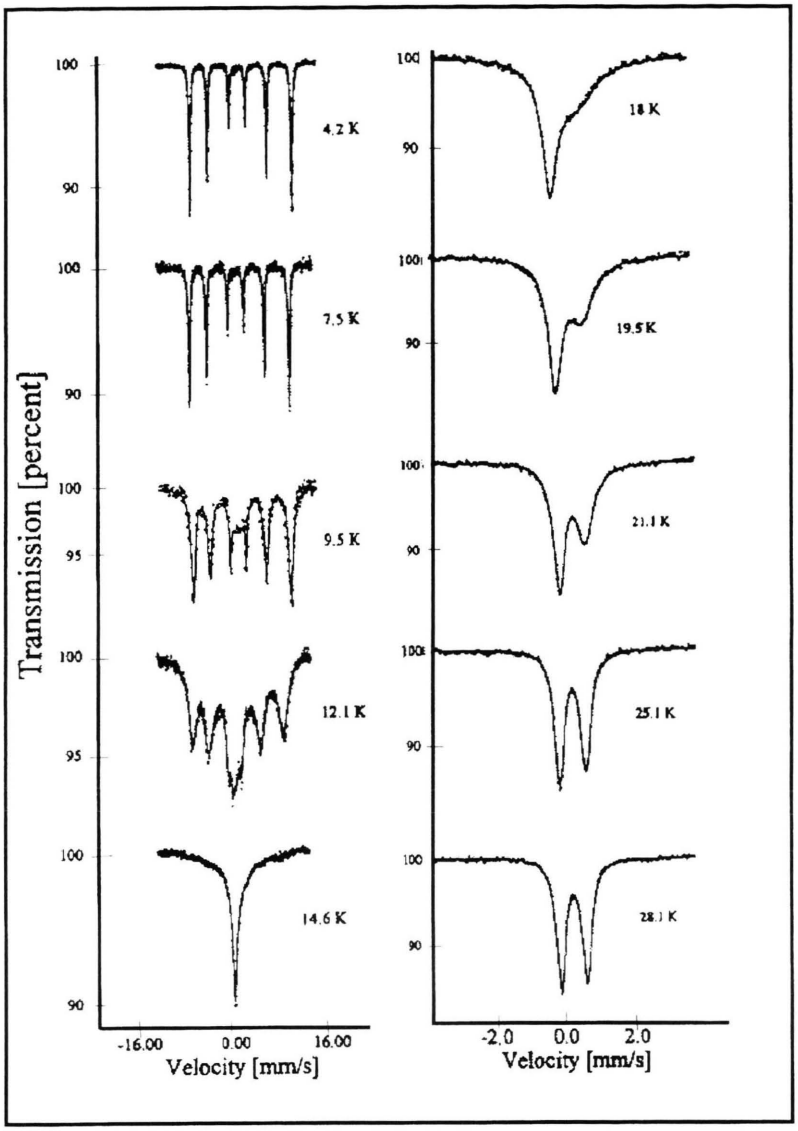

Fig. 1. Representative Mössbauer spectra for $(NH_4)_2Mn_{0.98}Fe_{0.02}F_5$. The continuous line represents a least-squares fit to the applied relaxation model of Blume and Tjon [34–36].

In our earlier papers it has been shown that this spin fluctuation rate, resulting from non-linear excitations, appears both in ferro- and antiferromagnetic Ising-like chain systems at temperatures roughly between T_c and $3T_c$, where T_c is the three-dimensional ordering temperature. The activation energy E_A, as determined from the electronic fliprate as a function of inverse temperature (see (8)), was systematically found to be twice the energy E_s of a single soliton, that is it corresponds to the energy of a soliton pair [46, 47]. This result is in contrast to the ideal gas description predicting the activation energy to be that of a single soliton. In the ideal soliton approximation [48] it is supposed that the solitons are present on the basis of entropy considerations, and their displacement is responsible for the spin fluctuations. Since the soliton pair excitations appear to be thermally activated, it is most probable that the coupling between the phonon bath and the spin system is responsible for their creation and annihilation. The present chain systems show spin-orbit coupling, which may provide for the thermal link between the phonon and the spin system [49].

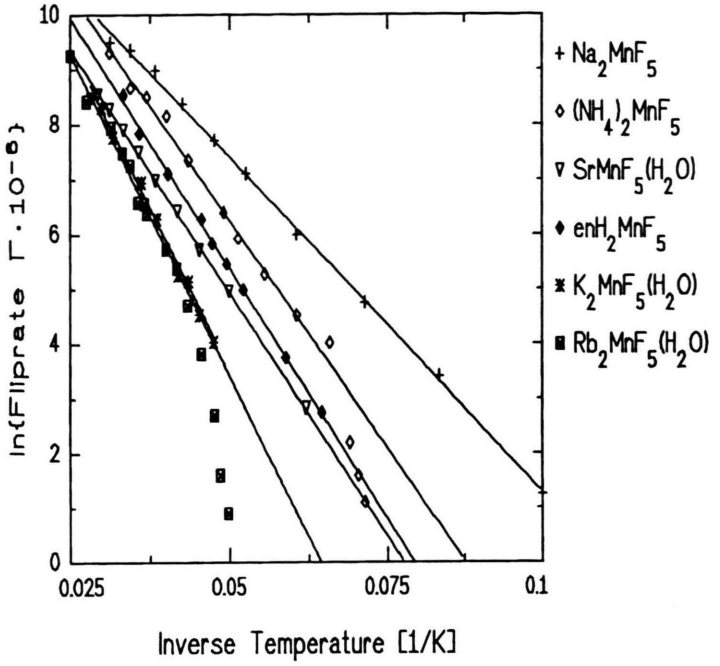

Fig. 2. Relaxation rate (fliprate) versus inverse temperature for $Na_2Mn_{0.98}Fe_{0.02}F_5$, $(NH_4)_2Mn_{0.98}Fe_{0.02}F_5$, $SrMn_{0.98}Fe_{0.02}F_5(H_2O)$, $enH_2Mn_{0.98}Fe_{0.02}F_5$, $K_2Mn_{0.98}Fe_{0.02}F_5(H_2O)$, and $Rb_2Mn_{0.99}Fe_{0.01}F_5(H_2O)$. The slopes of the exponentials were calculated by a least squares fit. Their values represent the activation energies which are to be compared with the soliton energy E_S.

The second subspectrum, a asymmetric doublet relaxes fast and shows a temperature independent relaxation rate. We had identified this subspectrum with the intra-band excitations discussed by Nagler et al. [50]. The level splittings in this soliton pair band are small with respect to the temperature, resulting in a fast relaxation behaviour. We remark that these rapid fluctuations have to be restricted to only parts of the chain during the characteristic Mössbauer time, since otherwise the slowly relaxing component would simply be not present. It is worthwhile to comment that the fast relaxing doublet disappears if a magnetic field is applied. This is expected, since an applied field polarizes the spins and lifts the degeneracy of their energy levels.

In Fig. 2 we present the relaxation rate versus inverse temperature for the ^{57}Fe doped compounds of the fluoromanganates(III) mentioned above. Additionally, we present up to now unpublished measurements for $SrMnF_5(H_2O)$, $BaMnF_5(H_2O)$ in Fig. 2 [21]. The slopes for the exponentials are $2E_S$. It follows from the plots of $\ln(\Gamma)$ vs. $1/T$ that the soliton energy E_S may be determined directly from Figure 2. The derived activations E_S/k are listed in Table 2.

The results obtained by the classical soliton theory (see (2)–(8)) are only strictly valid in the low temperature region ($T \to 0$) [16], since it requires the solitons not to interact (see above). The application of (7a) for higher temperatures (higher soliton density) is therefore rather questionable. For higher temperatures a boundary condition is, that the inverse correlation length $\xi^{-1}(T)$ for $T \to |J|\, S(S+1)/k$ turns continuously to an isotropic be-

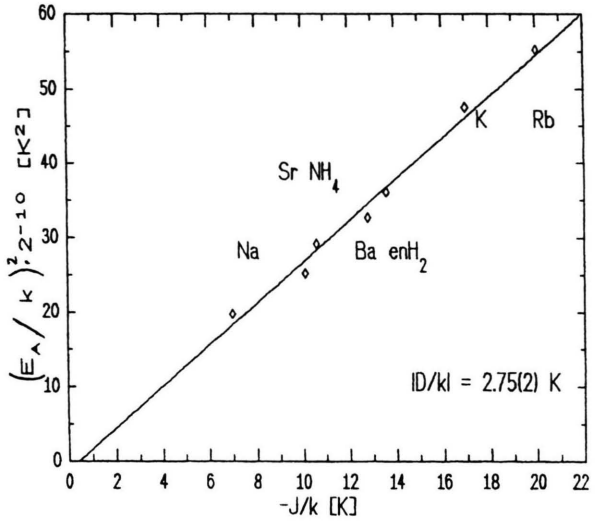

Fig. 3. The relationship between the activation energy $E_A=(2E_S)^2$ and the antiferromagnetic 1-d exchange constant $|J|$. From a linear least squares fit we derive from the classical soliton model $E_S=4S^2\ (|DJ|)^2$ the local anisotropy energy $|D/k|=2.75(3)$ K.

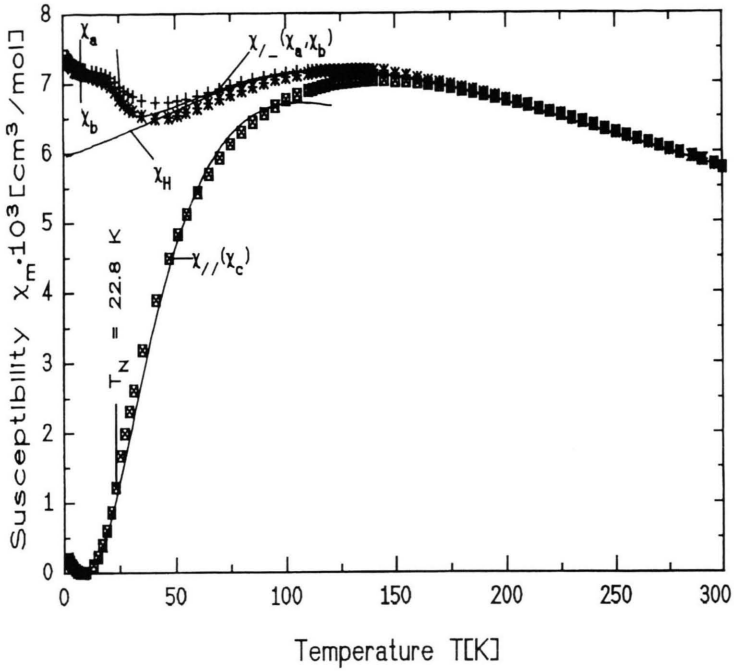

Fig. 4. Magnetic susceptibility in the three crystallographic axes vs. temperature for $Rb_2MnF_5(H_2O)$. The solid lines are calculated by the model given in the text with the parameters of the anisotropy constant $D/k = -2.95(3)$ K, the exchange constant $J/k = -20.1(3)$ K, the Néel temperature $T_N = 22.8(5)$ K, the spin canting angle $\varphi \equiv 0.0(5)°$, and the soliton energy $E_s/k = 117(3)$ K. The solid line of χ_H represents the solution for the isotropic Heisenberg model.

haviour predicted by the Heisenberg model [51, 52] and given by:

$$\xi^{-1} = -\ln\left[\coth\left\{\frac{2|J|S(S+1)}{kT} - \frac{kT}{2|J|S(S+1)}\right\}\right]. \quad (7b)$$

From this simple model of isotropic spin interactions we had calculated the exchange constants near $T(\chi_{max})$ many years ago [3]. Figure 3 shows now the correlation between the activation energy $(2E_s)^2$ derived from the classical soliton model and the antiferromagnetic 1-d exchange constants J (see Table 2). From a linear least squares fit (Fig. 3) we derive the local anisotropy energy $|D/k| = 2.75(3)$ K.

We can test the predictions of the soliton theory (see (2)–(8)) by calculating the magnetic susceptibilities from the temperature dependence of the inverse correlation length $\xi^{-1}(T)$ and compare these with experimental results obtained from magnetic measurements on single crystals of the fluoromanganates(III).

Magnetic Susceptibility along the Chain-direction

In Figs. 4, 5, and 6 we present the magnetic susceptibilities as examples for single crystals of Na_2MnF_5, $(NH_4)_2MnF_5$, and $Rb_2MnF_5(H_2O)$. Previously [9] we reported magnetic investigations on single crystals of $(NH_4)_2MnF_5$, $(NH_4)_2Mn_{0.98}Fe_{0.02}F_5$, and enH_2MnF_5 [10]. The magnetic studies on single crystals of Na_2MnF_5 (15 mg), $(NH_4)_2MnF_5$ (40 mg), enH_2MnF_5 (12 mg), $K_2MnF_5(H_2O)$ (11 mg), and $Rb_2MnF_5(H_2O)$ (20 mg) were performed with a SQUID magnetometer [53] in the temperature range 1.7–330 K and external fields up to ±55 kG. The experimental procedure for determining the Néel temperatures has been described in detail in [12]. These transition temperatures T_N are listed in Table 2.

The experimental $\chi_{||}(T)$ data for Na_2MnF_5, $(NH_4)_2MnF_5$, and $Rb_2MnF_5(H_2O)$ represent the susceptibilities along the chain directions a, b, and c, and $\chi_\perp(T)$ are the perpendicular susceptibilities along the b and c or a and c or a and b axes, respectively. In the 3-d ordered magnetic phase the hierarchy of the $\chi_\perp$ components is for example as follows: $\chi_b > \chi_c$ for Na_2MnF_5, $\chi_a > \chi_c$ for $(NH_4)_2MnF_5$, and $\chi_a > \chi_b$ for $Rb_2MnF_5(H_2O)$.

If the temperature dependence of the correlation length is known (see (7a)), the static pair-correlation function for the compounds in question may be determined. According to Fisher [51, 54] the correlation function is given as

$$C_r(T) = \langle S_0^z S_r^z \rangle = \frac{S(S+1)}{3} \cdot \exp(-\xi^{-1}), \quad (9)$$
$$(r = 0, 1, 2, \ldots, \infty),$$

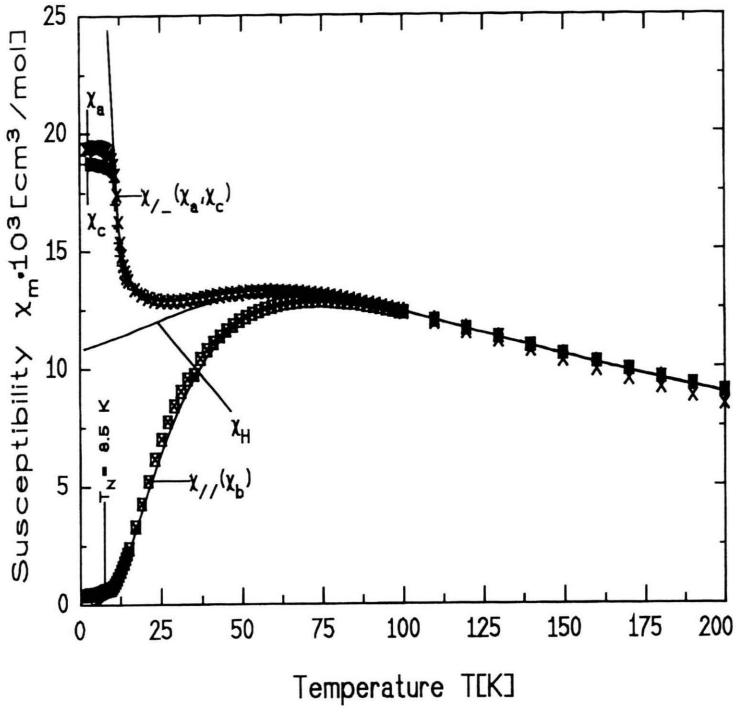

Fig. 5. Single crystal magnetic susceptibility of $(NH_4)_2MnF_5$ for the three crystallographic axes vs. temperature. The curves are calculated from the present model. The obtained parameters are the anisotropy constant $D/k = -2.85(3)$ K, the exchange constant $J/k = -10.6(1)$ K, the Néel temperature $T_N = 8.5(2)$ K, the spin canting angle $\varphi \cong 4.6(2)°$, and the soliton energy $E_s/k = 83(2)$ K. The solid line of χ_H represents the solution for the isotropic Heisenberg model.

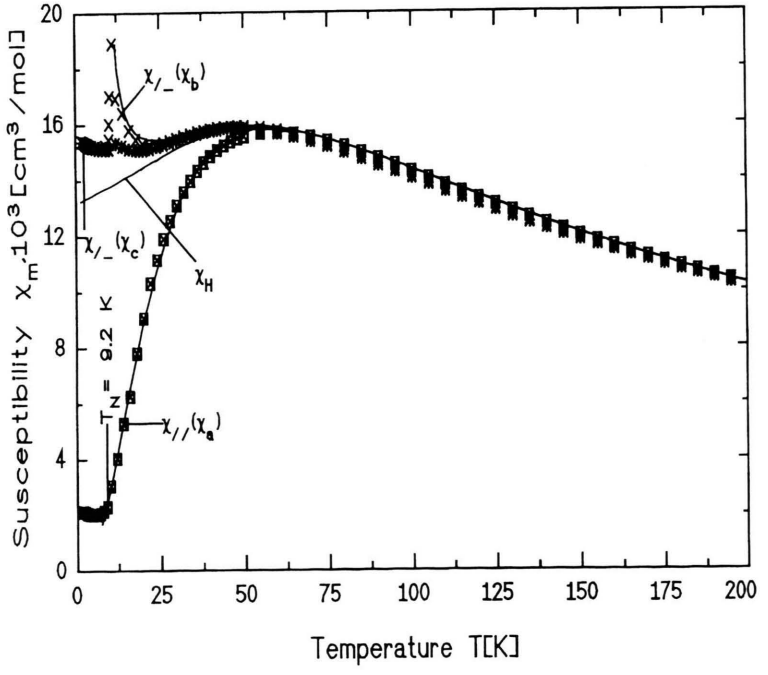

Fig. 6. Single crystal magnetic susceptibility of Na_2MnF_5 for the three crystallographic axes vs. temperature. The solid lines are calculated with the parameters of the anisotropy constant $D/k = -2.85(4)$ K, the exchange constant $J/k = -8.8(2)$ K, the Néel temperature $T_N = 9.2(2)$ K, the spin canting angle $\varphi \cong 5(1)°$, and the soliton energy $E_s = 70(3)$ K. The solid line χ_H represents the solution for the isotropic Heisenberg model.

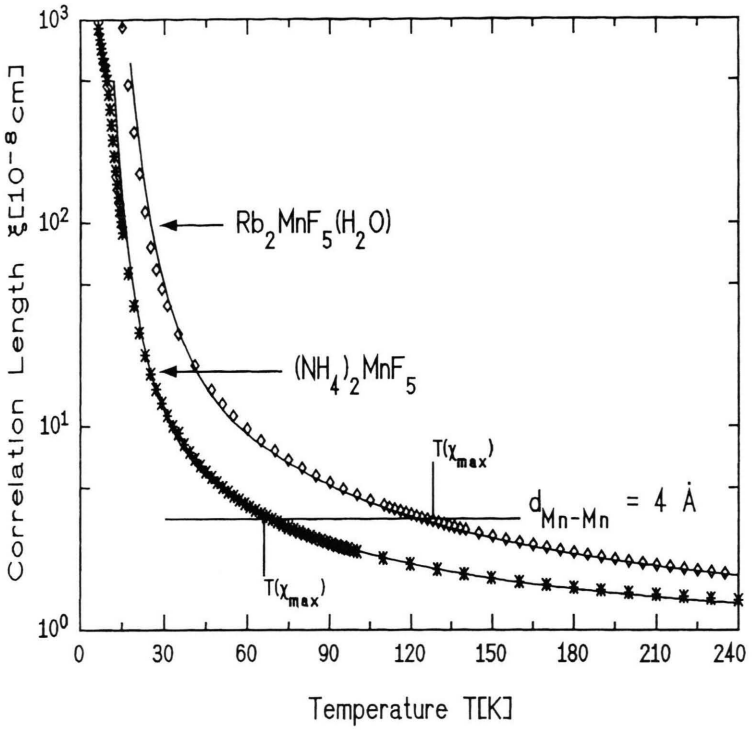

Fig. 7. Temperature dependence of the correlation lengths $(NH_4)_2MnF_5$ and $Rb_2MnF_5(H_2O)$. At the average shortest metal–metal distance of 4 Å the points of intersection correspond to the values of $T(\chi_{max})$.

where (8) describes the degree of correlation between a reference spin S_0 and a varying (fluctuating) spin S_r at the distance r.

According to Steiner et al. [42] the susceptibility of a 1-d antiferromagnet follows

$$\chi_{\parallel}(T) = \frac{N g^2 \mu_B^2 S(S+1)}{3kT} \cdot \frac{1 - \exp\left\{-\frac{b_0}{\xi}\right\}}{1 + \exp\left\{-\frac{b_0}{\xi}\right\}}. \quad (10)$$

For $\xi \to 0$ and $T \to J S(S+1)/k \approx T(\chi_{max})$, $\chi_{\parallel}$ smoothly approaches the Curie law. The term $(S(S+1)/3) \cdot \exp(-1/\xi)$ represents the correlation function $\langle S_0^z S_r^z \rangle$ of (9). b_0 is the shortest metal–metal distance along the chain direction. According to (7a) we find the relation

$$\exp\left\{-\frac{b_0}{\xi}\right\} = \exp\left\{-2 b_0 \sqrt{\frac{8}{\pi}} \sqrt{\frac{D}{J}} \sqrt{\frac{E_s}{kT}} \cdot \exp\left\{\frac{-E_s}{kT}\right\}\right\}. \quad (11)$$

If we insert this expression, derived from the soliton model (see (7a)), in (10), the calculation yields the parallel component of the magnetic susceptibility, which is represented by a solid line in Figs. 4–6 and has been labeled $\chi_{\parallel}$. For Na_2MnF_5 the simulation of the magnetic susceptibility $\chi_{\parallel}$ by (9) is excellent. For $(NH_4)_2MnF_5$ the theoretical values according to (10) come close to the maximum of the magnetic susceptibility at $T = T(\chi_{max}) \cong S(S+1)|J|/k \cong 63$ K. For $Rb_2MnF_5(H_2O)$ with $T(\chi_{max}) \cong 128$ K the correlation function used in (10) breakes down for temperatures higher than 60 K.

For comparison we have also plotted the results for the magnetic susceptibility χ_H according to the Heisenberg-model (see (7b)) in Figs. 4, 5, and 6. It is valid for $T > T(\chi_{max})$ since the effective spin-correlations along the chain vanish at $T(\chi_{max})$. The correlation length ξ for temperatures $T \cong |J| S(S+1)/k$ is smaller than the average intermetallic Mn^{3+}-Mn^{3+} distance of 4 Å. This is demonstrated in Fig. 7 for the compounds of $(NH_4)_2MnF_5$ and $Rb_2MnF_5(H_2O)$, where the calculated correlation lengths of the classical soliton model (7a) are plotted as functions of temperature T. The parameters D, J, and E_s found from the least squares fit are given in Table 2. As starting parameters we used D and E_s derived from our Mössbauer relaxation spectra.

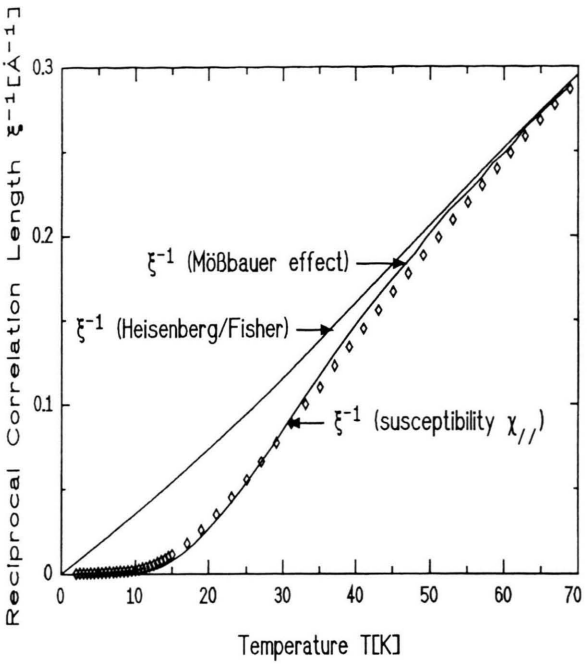

Fig. 8. Reciprocal correlation length $1/\xi$ for $(NH_4)_2MnF_5$ vs. T. The lower solid line is the solution (7a) from the classical soliton model. The measuring points of $1/\xi$ were recalculated from single-crystal susceptibility measurements (11)–(12). Additionally, the solution for the 1-d Heisenberg model is shown.

Additionally, we have recalculated the correlation lengths from (9) using the relation

$$\xi^{-1} = \ln\left\{\frac{1-A}{1+A}\right\} \quad \text{with} \quad A = \frac{3\chi_{\|}\, kT}{N g^2 \mu_B^2 S(S+1)}. \tag{12}$$

Inserting in (12) the measured values $\chi_{\|}$, we obtain the temperature dependence of ξ^{-1} derived from the magnetic susceptibility. These calculated values were inserted in Fig. 8 as points. The comparison confirms that the analytical form $\xi^{-1}(T)$ derived from the spin dynamics is not very different and describes $\chi_{\|}$ nicely, at least in the low temperature region (Figure 8). For large temperatures $T \to T(\chi_{\max})$ the analytical form of (7a) failed, especially for compounds with large $T(\chi_{\max})$ values.

Figures 4, 5, and 6 demonstrate that the correlation lengths determined on the basis of the soliton model describe the parallel component of the magnetic susceptibility correctly for temperatures below 60 K.

For higher temperatures ($T \geq 60$ K) where the wall separation is comparable to the wall width, that is $\xi \approx b_0$, one has to take interactions between the solitons as well as simultaneous excitations of solitons and antisolitons (excited pair-states) into account [16, 18, 46, 47]. In this temperature regime, the soliton velocity v_s is possibly slowed down due to the soliton–antisoliton and soliton–phonon interactions [16]. This demonstrates that at higher temperatures the classical soliton model breaks down. It is worth noting that for high temperatures within the 1-d phase the quality of fitting can be increased by assuming that the soliton velocity is nearly temperature independent.

A series expansion in powers of (kT/E_s) after Sasaki and Tsuzuki [55], which accounts for the existence of a magnon as well as a soliton contribution, does not improve the description of the temperature dependence of correlation lengths $\xi_{\|}$ or $\chi_{\|}$ in the high temperature region.

Griffiths [56] has suggested a perturbation procedure by which a semiquantitative description to the axial anisotropy might be built upon Fisher's classical Heisenberg model [51]. From his evaluation of the higher-order spin-correlation functions Smith et al. [52] and Kida et al. [26] derived for $\chi_{\|}$ and $\chi_{\perp}$ an analytical expression. This expression, however, is in contradiction to our results and to the requirement of an exponential increase in the correlation length $\xi_{\|}$ if one approaches absolute zero, or that for $T \to 0$ the static correlation function should approach unity. The perturbation procedure by Griffiths is expected to be valid only where the anisotropy $\chi_{\perp} - \chi_{\|}$ is not large compared to the average susceptibility $(\chi_{\|} + 2\chi_{\perp})/3$, i.e. in a certain region below $T(\chi_{\max})$ within the 1-d antiferromagnetic phase.

Since the pure 1-d antiferromagnet has no finite T_N, irrespective of the symmetry of the Hamiltonian, the observed transition is due to the weak interchain coupling J'. Nevertheless, the value of T_N is directly related to the 1-d correlation length $\xi_{\|}(T)$ along the chain, as follows from the relation

$$kT_N \cong |J'|\, S(S+1) \cdot \xi_{\|}(T_N), \tag{13}$$

which equates the thermal energy at T_N to the interaction energy between correlated chain segments on adjacent chains [45]. Because the Néel-temperatures T_N of 8.5(2) and 22.5(3) K and the 1-d correlation lengths $\xi^{1D}(T_N)$ are known from (7a), the inter-chain exchange energies $|J'/k|$ for $(NH_4)_2MnF_5$ and $Rb_2MnF_5(H_2O)$ result to $2.7(3) \cdot 10^{-4}$ K and $1.6(3) \cdot 10^{-2}$ K, respectively. The ratio $|J'|/|J| = R$, which is a measure for the one-dimensionality of a magnet, results to $2.6 \cdot 10^{-5}$ (NH_4) and $8.3 \cdot 10^{-4}$ (Rb).

In Table 2 we placed together the local anisotropy D, 1-d exchange constant J, soliton energy E_s, inter-chain exchange constant J', and Néel-temperature T_N derived from our calculations.

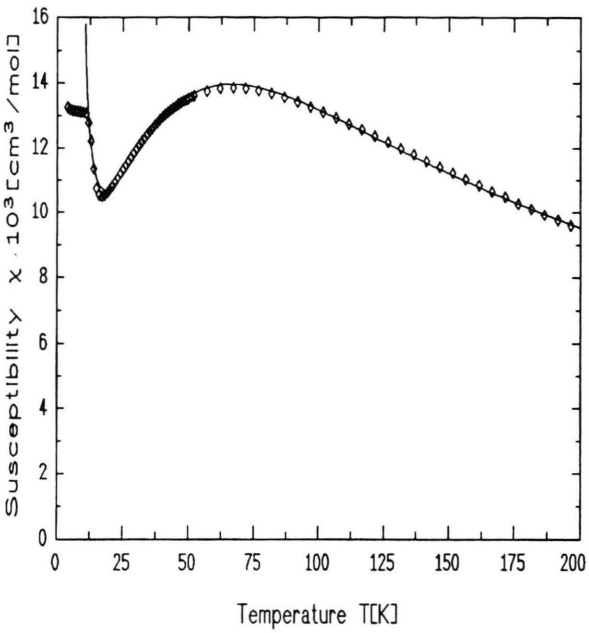

Fig. 9. Fitting of the magnetic susceptibility of the powder sample of $(NH_4)_2MnF_5$ with the relation (15) described in the text. As starting parameters the anisotropy constant and the Néel temperature were fixed and the susceptibility was varied as a function of J and φ. Finally, the susceptibility was calculated with the parameters of the anisotropy constant $D/k = 2.85(5)$ K, the exchange constant $J/k = 10.4(2)$ K, the soliton energy $E_s/k = 85(2)$ K, the spin canting angle $\varphi = 4.6°$, and the Néel temperature $T_N = 8.5(1)$ K.

Magnetic Susceptibility Perpendicular to the Chain-direction

From our single crystal measurements we find, as mentioned above, that the spins are nearly antiparallel to the z axis (chain direction), but they have small canted components along the x or y axes (perpendicular to the chain direction) in the ordered state, which produce a weak ferromagnetism. Previously, magnetic measurements on a single crystal of $(NH_4)_2MnF_5$ with the transverse detection unit of our SQUID system [53] showed that the ferromagnetic moment lies within the a, c plane for $T < T_N$ [21]. The canting angle φ is caused by the local anisotropy producing a different preferential direction for the moments which are on different sublattices. This mechanism occurs when the local arrangement of the atoms around the sites of the magnetic ions are tilted with respect to each other.

The direction of local anisotropy for each sublattice is assumed to make an angle $\delta = (180° - \gamma)/2$ with the positive or negative z axis, where γ represents the bridging angle (Table 1). If the preferred direction due to the anisotropy is the same for both sublattices ($\delta = 0$), the canting angle φ is evidently equal to zero. An increase of δ also increases the canting angle. If, on the other hand, the exchange interaction J is zero, it is easily seen that $\delta = \varphi$.

To describe the spin behaviour one has, as mentioned above, to solve the Hamiltonian of a magnetic chain for orthorhombic symmetry. Due to the isotropy within the plane perpendicular to the chain axis ($E \cong 0$) we can construct the following expression for the susceptibility perpendicular to the chain axis. According to Moriya [57] the magnetic susceptibility of a canted system may be described by the sum of two contributions, namely an antiferromagnetic and a ferromagnetic part. Each of the contributions must be multiplied with an appropriate factor to take the value of the susceptibility component along the particular axis into account. For our description of the experimental susceptibility data on the weak ferromagnetic chain compounds, we used the correct theoretical expression for the 1-d Heisenberg model, multiplied with the factor $(1 - \sin^2\varphi)$ [57]. Following Moriya [57], the ferromagnetic component can be described by a term $C/(T - T_N)$ multiplied with the factor $\sin^2\varphi$, where C is the Curie constant. In our case, for $\chi_\perp$ it follows that

$$\chi_\perp = \frac{N g^2 \mu_B^2 S(S+1)(1-\sin^2\varphi)}{3kT} \frac{1-\exp\{\xi_H^{-1}\}}{1+\exp\{\xi_H^{-1}\}} + \frac{N g^2 \mu_B^2 S(S+1)}{3k(T-T_N)} \sin^2\varphi , \tag{14}$$

where ξ_H^{-1} represents the inverse correlation length (see (9)) in the Heisenberg model. The Figs. 4, 5, and 6 show the results for best fits of (14) to the experimental data for the perpendicular component of the magnetic susceptibility $\chi_\perp$. For Na_2MnF_5, $(NH_4)_2MnF_5$ and $Rb_2MnF_5(H_2O)$ values of $T_N = 9.5$ K, 8.5 K or 22.5 K and $\varphi = 5.1°$, 4.8° or 0.4° have been taken into account.

Considering (10) and (14), we can derive an expression calculating the magnetic susceptibilities of powder samples as is demonstrated for the case of $(NH_4)_2MnF_5$ in Figure 9. The average magnetic susceptibility may then be written as

$$\chi_{\text{Powder}} = \frac{1}{3}(\chi_\parallel + 2 \cdot \chi_\perp) = \frac{N g^2 \mu_B^2 S(S+1)}{3k} \frac{1}{3} \left\{ \frac{1}{T} \cdot \frac{1-\exp(\xi^{-1})}{1+\exp(\xi^{-1})} + \left(\frac{2}{T}(1-\sin^2\varphi) \frac{1-\exp(\xi_H^{-1})}{1+\exp(\xi_H^{-1})} + 2\frac{\sin^2\varphi}{T-T_N} \right) \right\}. \tag{15}$$

Fixing as starting parameters the Néel temperature T_N and the exchange constant J, the adjustable parameters are the anisotropy constant D, the soliton energy E_s, and the spin canting angle φ. Finally we found from the best fit of (15) to the data: of $(NH_4)_2MnF_5$: $D/k = -2.85(5)$ K, $J/k = -10.4(2)$ K, $E_s = 85(3)$ K, and $\varphi = 4.5°$ (see Figure 9). These results are in excellent agreement with our single crystal study.

In order to check our results discussed above we have started to perform inelastic neutron scattering experiments at the Hahn-Meitner-Institute at BER-II in Berlin to determine the magnetic linear [28] and non-linear excitations of $(NH_4)_2MnF_5$. However, the inelastic magnetic signals were weak and strongly hidden by the large incoherent background caused by the hydrogen atoms. After the availability of large deuterated single crystals (1.5 g) of good quality, which have been characterized crystallographically by elastic neutron diffraction [27], the study of inelastic neutron scattering has been performed on the compound $(ND_4)_2MnF_5$. The results, which will be published elsewhere [58], are in excellent agreement with our investigations above.

Acknowledgements

We thank W. Massa for many helpful discussions. Supports of this work by the Bundesministerium für Bildung, Wissenschaft, Forschung und Technologie, and the Fonds der Chemischen Industrie are gratefully acknowledged.

[1] D. Babel and A. Tressaud, "Inorganic Solid Fluorides", Chemistry and Physics, Materials Science Series, ed. by P. Hagenmuller, Academic Press, New York 1985.
[2] W. Massa and D. Babel, Chem. Reviews **88**, 275 (1988).
[3] J. Pebler, W. Massa, H. Lass, and B. Ziegler, J. of Solid State Chemistry **71**, 87 (1987).
[4] W. Massa, M. Molinier, and J. Pebler, J. of Fluorine Chemistry **72**, 171 (1995).
[5] U. Bentrup, L. Schröder, and W. Massa, Z. Naturforsch. **47b**, 789 (1992).
[6] J. Pebler and D. Babel, Organic and Inorganic Low-Dimensional Crystalline Materials, NATO ASI Series, Plenum Press, New York 1987.
[7] W. Massa, J. Pebler, F. Hahn, and D. Babel, "Organic and Inorganic Low-Dimensional Crystalline Materials", NATO ASI Series, Plenum Press, New York 1987.
[8] J. Pebler, Inorg. Chemistry **28**, 1038 (1989).
[9] C. Frommen and J. Pebler, Hyperfine Interactions, **96**, 51 (1995).
[10] C. Frommen, L. Schröder, U. Bentrup, W. Massa, and J. Pebler, Z. Naturforsch. **50b**, 1227 (1995).
[11] W. Massa, M. Molinier, and J. Pebler, J. of Fluorine Chemistry **72**, 171 (1995).
[12] C. Frommen, M. Mangold, and J. Pebler, Z. Naturforsch. **51a**, 939 (1996).
[13] L. J. de Jongh (Ed.), "Magnetic Properties of Layered Transition" Metal Compounds, Kluwer Academic Publishers, Dordrecht 1990, and references therein.
[14] L. J. de Jongh, "Magneto-Structural Correlations in Exchange Coupled Systems", NATO ASI Series, D. Seidel Publishing Company, Dordrecht 1983.
[15] C. E. Johnson, "One Dimensional Magnetism", from: Mössbauer Spectroscopy Applied to Inorganic Chemistry, Vol. 1, Gary Long ed., Plenum Publishing Corporation, New York 1984.
[16] H. J. M. de Groot, Thesis, Leiden, The Netherlands 1986.
[17] R. C. Thiel, H. de Graaf, and L. J. de Jongh, Phys. Rev. Lett. **47**, 1415 (1981).
[18] H. H. A. Smit, Thesis, Leiden, The Netherlands 1988.
[19] C. Frommen, Diplomarbeit, Marburg 1991.
[20] M. Mangold, Diplomarbeit, Marburg 1994.
[21] C. Frommen, Thesis, Marburg 1994.
[22] D. Reinen and C. Friebel, Structure and Bonding **37**, 1 (1979).
[23] I. B. Bersuker, "Jahn-Teller-Effect and Vibronic Interactions in Modern Chemistry", Plenum Press, New York 1984.
[24] W. Massa, Acta Crystallogr. Sect. **C42**, 644 (1986).
[25] D. R. Sears and J. L. Hoard, J. Chem. Phys. **50**, 1066 (1969).
[26] J. Kida and T. Watanabe, J. Phys. Soc. Japan **34**, 952 (1973).
[27] W. Massa, W. Paulus, M. Mangold, and J. Pebler, Elastic Neutron Study, to be published 1999.
[28] M. Steiner, M. Winkelmann, M. Baehr, D. Hohlwein, A. Krimmel, C. Frommen, M. Mangold, and J. Pebler, Physica **B241**, 555 (1998).
[29] A. J. Edwards, J. Chem. Soc. A, 2653 (1971).
[30] M. Molinier, Thesis, University of Marburg 1993.
[31] P. Bukovec and V. Kaucic, Acta Crystallogr., Sect. **B34**, 3337 (1978).
[32] H. Thomas, "Theory of Jahn-Teller Transitions", in: Electron-Phonon Interactions and Phase Transitions, ed. by T. Riste, Plenum Press, New York 1977.
[33] J. M. Dance, private communication (1987).
[34] M. Blume and J. A. Tjon, Phys. Rev. **B165**, 446 (1968).
[35] M. Blume and J. A. Tjon, Phys. Rev. **B174**, 351 (1968).
[36] J. Pebler, J. Phys. Status Solidi **A78**, 589 (1983).
[37] H. J. Mikesha and M. Steiner, Advances in Physics **40**, 191 (1991).
[38] J. P. Boucher, Hyperfine Interactions **49**, 423 (1989).
[39] J. Villain, Physica **79B**, 1 (1975).
[40] K. Maki, Phys. Rev. **214**, 335 (1981).
[41] H. J. Mikeska, J. Appl. Phys. **52**, 1950 (1981).
[42] M. Steiner, J. Villain, and C. G. Windsor, Adv. Phys. **25**, 87 (1976).
[43] M. Steiner, "Ordering In Strongly Fluctuating Condensed Matter Systems", T. Riste ed., Plenum Publishing Corporation, New York 1980.
[44] J. K. Kjems and M. Steiner, Phys. Rev. Lett. **41**, 1137 (1978).
[45] L. J. de Jongh, J. Appl. Phys. **53**, 8018 (1982).
[46] M. Elmassalami, Thesis, Leiden, The Netherlands 1989.
[47] M. Elmassalami, H. H. A. Smit, H. de Groot, R. C. Thiel, and L. J. de Jongh, Proc. in Phys. 23, "Magnetic Excitations and Fluctuations II", eds. U. Balucani, S. W. Lovesey, M. G. Rasetti, and V. Tognetti, Springer-Verlag, Berlin 1987, p. 178.

[48] A. R. Bishop, J. A. Krumhansl, and S. E. Trullinger, Physica **1D**, 1 (1980).
[49] E. Orbach, Proc. Roy. Soc. London **A264**, 458 (1961).
[50] S. E. Nagler, W. J. L. Buyers, R. L. Armstrong, and B. Briat, Phys. Rev. **B28**, 3873 (1983).
[51] M. E. Fisher, Amer. J. Phys. **32**, 343 (1964).
[52] T. Smith and S. A. Friedberg, Phys. Rev. **176**, 660 (1968).
[53] from QUANTUM DESIGN, San Diego, U.S.A. 1991.
[54] L. J. de Jongh and A. R. Miedema, "Experiments on Simple Magnetic Model Systems", Taylor and Francis LTD, London 1974.
[55] K. Sasaki and T. Tsuzuki, Sol. St. Com. **41**, 521 (1982); K. Sasaki and T. Tsuzuki, J. Magn. Mater. **31–34**, 1283 (1983).
[56] R. B. Griffiths, private communication in [51, 52].
[57] T. Moriya, Phys. Rev. **120**, 91 (1960).
[58] A. Krimmel, R. van de Kamp, C. Frommen, M. Mangold, and J. Pebler, to be published in Phys. Rev. B (1999).